Hindawi
International Journal of Aerospace Engineering
Volume 2019, Article ID 2580865, 13 pages
https://doi.org/10.1155/2019/2580865

Research Article

Development of Pogo Pin-Based Holding and Release Mechanism for Deployable Solar Panel of CubeSat

Shankar Bhattarai,[1] Hongrae Kim,[2] Sung-Hoon Jung,[3] and Hyun-Ung Oh[1]

[1]*Space Technology Synthesis Laboratory, Department of Aerospace Engineering, Chosun University, Gwangju, Republic of Korea*
[2]*Soletop Co. Ltd., 409 Expo-ro, Yuseong-gu, Daejeon, Republic of Korea*
[3]*Agency for Defense Development, Yuseong-gu, Daejeon, Republic of Korea*

Correspondence should be addressed to Hyun-Ung Oh; ohu129@chosun.ac.kr

Received 15 December 2018; Accepted 17 March 2019; Published 5 May 2019

Academic Editor: Santiago Hernández

CubeSats are revolutionary to the space industry and are transforming space exploration which enables the next generation of scientists and engineers to complete all phases of space missions. Deployable solar panels have been widely used for the generation of enough power in CubeSats due to their limited volume area for solar cell integration. In general, the cable cutting release mechanism have been used in 1U-3U small satellites because of its simplicity and low cost. However, this mechanism has a low constraint force and is unable to apply constraints along the in-plane and out-of-plane directions. In this study, for the improvement of the conventional cable cutting mechanism, a spring-loaded pogo pin-based nichrome burn wire holding and release mechanism (HRM) was proposed and fabricated. The pogo pin constitutes an immensely attractive function for the holding and release mechanism of solar panels because it works as an electrical interface to provide power, a separation spring to initiate the reaction force to deploy the panels, and a status switch to determine deployments. In addition, the proposed mechanism guarantees the loading capability along the in-plane and out-of-plane directions of solar panels, the synchronous release of multiple panels, and a handling simplicity that differentiates it from the conventional mechanism. The design feasibility, structural safety, and reliability of the mechanism were verified through functionality tests and launch and on-orbit environmental tests. The proposed pogo pin-based holding and release mechanism would be equally applicable for other CubeSat deployable appendages.

1. Introduction

In 1957, the Soviet Union officially initiated the modern space age by launching the Sputnik satellite into low Earth orbit. This step was quickly followed by the successful launches of the Explorer 1 and Vanguard 1 satellites [1]. During the last decade, the size of satellites launched into the space has been decreased significantly, whereas their capabilities increased, due to the miniaturization of electronics and the increase in the system integration density. The use of small satellites offers several benefits such as a decrease in the launch cost and development time. The basic CubeSat configuration, referred to as 1U, has a standard dimension of $10 \times 10 \times 10$ cm^3 and an approximate mass of 1.33 kg, although larger configurations are also available. Although the size of microprocessors and computing technology continue to shrink in size, the power requirements for components remain steady. Moreover, payloads and data transmission capabilities are also limited if the power generation is insufficient. To enhance the capability of a CubeSat, deployable solar panels are required, which would increase the surface area of a CubeSat for the installation of solar cells and would help orient the panels to face perpendicular to the sun for effective power generation. When the sun is orthogonal to the solar panels, the power generation performance would increase 160% to 400% with respect to the body-mounted solar panels [2]. This significantly increases the output power of the solar cells. An increase in the power generation of a CubeSat can increase its potential because data collection, data transmission, and data processing are

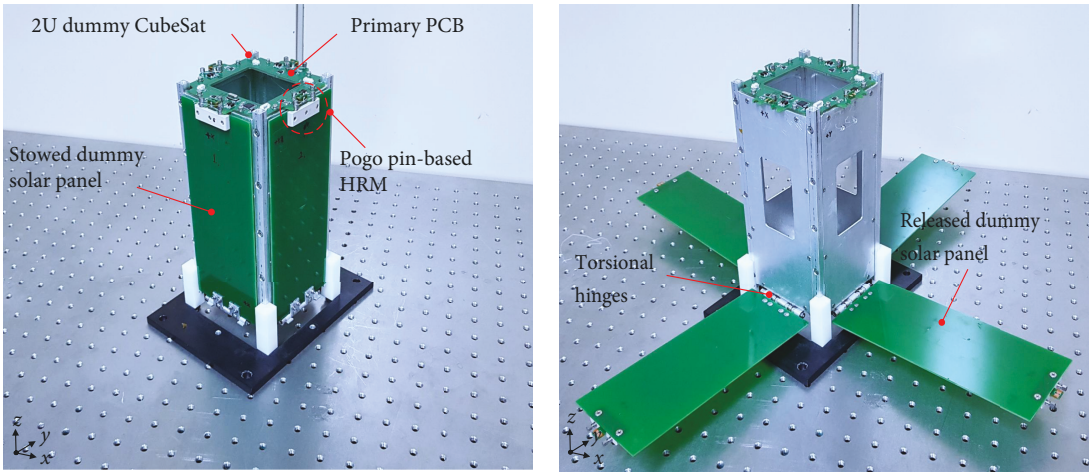

(a) (b)

Figure 1: Configurations of pogo pin HRM in a 2U dummy CubeSat: (a) stowed configuration and (b) deployed configuration.

dependent on the power capacity. Consequently, the power capacity of a CubeSat is as important as ever for a given CubeSat. Several studies have been carried out to maximize power generation [3, 4] and different solutions have been investigated to optimize the solar panel configuration, including the possibility of deploying solar arrays from the surface of the CubeSat [5, 6].

Several holding and release mechanisms have been developed and used to hold and release the deployable solar panels of a CubeSat [7, 8]. In commercial satellites and aerospace engineering, pyrotechnic devices have been used in the HRMs. A high-frequency pyroshock may induce an unexpected shock level and constitutes even more critical challenges for small satellites, as their electrical components are closely arranged due to their limited volume. To overcome the drawbacks of the pyrotechnical mechanism in pico-class satellites, several types of nonexplosive devices made by shape memory alloys (SMA) have been designed and used in CubeSat applications [9, 10]. However, these nonexplosive SMA actuators are not the best choice for CubeSats due to their high cost and increased weight. Therefore, a nichrome burn wire cutting method has been extensively used for the release of mechanical constraints on the deployable appendages of a CubeSat due to its simplicity and low cost. The mechanical constraint was released by cutting the nylon cable triggered by burn resistors. Thurn et al. [11] developed a burn wire release mechanism to release the tether deployment system. The mechanism utilized a compression spring system to apply a force and stroke to the nichrome burn wire to ensure a safer release. They conducted functional performance tests in a vacuum, and the test results indicated a shorter cut time of the mechanism in the vacuum when compared with that in air. However, this design has a very low constraint force and is unable to constrain along the in-out plane direction. Oh and Lee [12] developed a separation nut-type HRM based on the nichrome burn wire cutting, with several advantages, including an increased load capacity and negligible shock; the constraint force of nylon cable winding was released by cutting the nylon cable through a nichrome burn wire. The effectiveness of the design was verified by conducting a functionality test and static load tests under qualification temperature conditions on a demonstration model of the mechanism. Moreover, by realizing the significance of the nylon cable cutting release mechanism in pico-class satellites, Park et al. [13] proposed a novel deployable solar panel mechanism using spring-loaded pogo pins. The feasibility of the mechanism was evaluated by functional tests under various test conditions, such as different input voltages, different numbers of tightening nylon wires, and various temperature ranges. The basic functional test results confirm that the spring-loaded pogo pin constitutes an attractive function for a holding and release mechanism because it works as an electrical interface to provide power to the burn resistor, which is mounted on the burn resistor PCB of the solar panels. In addition, it can establish a temporal electrical connection and it also acts as a status switch to confirm the solar panel deployment status. However, in order to employ a pogo pin-based HRM in a real-time CubeSat mission, the mechanism should be qualified under severe launch and on-orbit thermal vacuum (TV) environments.

In this work, as an extension of a previous research [13], the electrical interface of a pogo pin-based HRM was redesigned and it was manufactured as a qualification model for use in actual space applications. The qualification model of the proposed HRM was subjected to launch vibration and TV environment tests. The modified electrical design was implemented on a primary printed circuit board (PCB), which also provides a mechanical interface to constrain the out-of-plane directional movement of the deployable solar panel. The modified PCB was used for the input power supply for each of the pogo pins, which reduced the risk of electrical malfunctions and increased the reliability of the mechanism. Moreover, the voltage was measured using a microcontroller unit (MCU) attached to the circuit, to help determine the deployable status of each of the solar panels. The newly proposed design was verified through the qualification level of

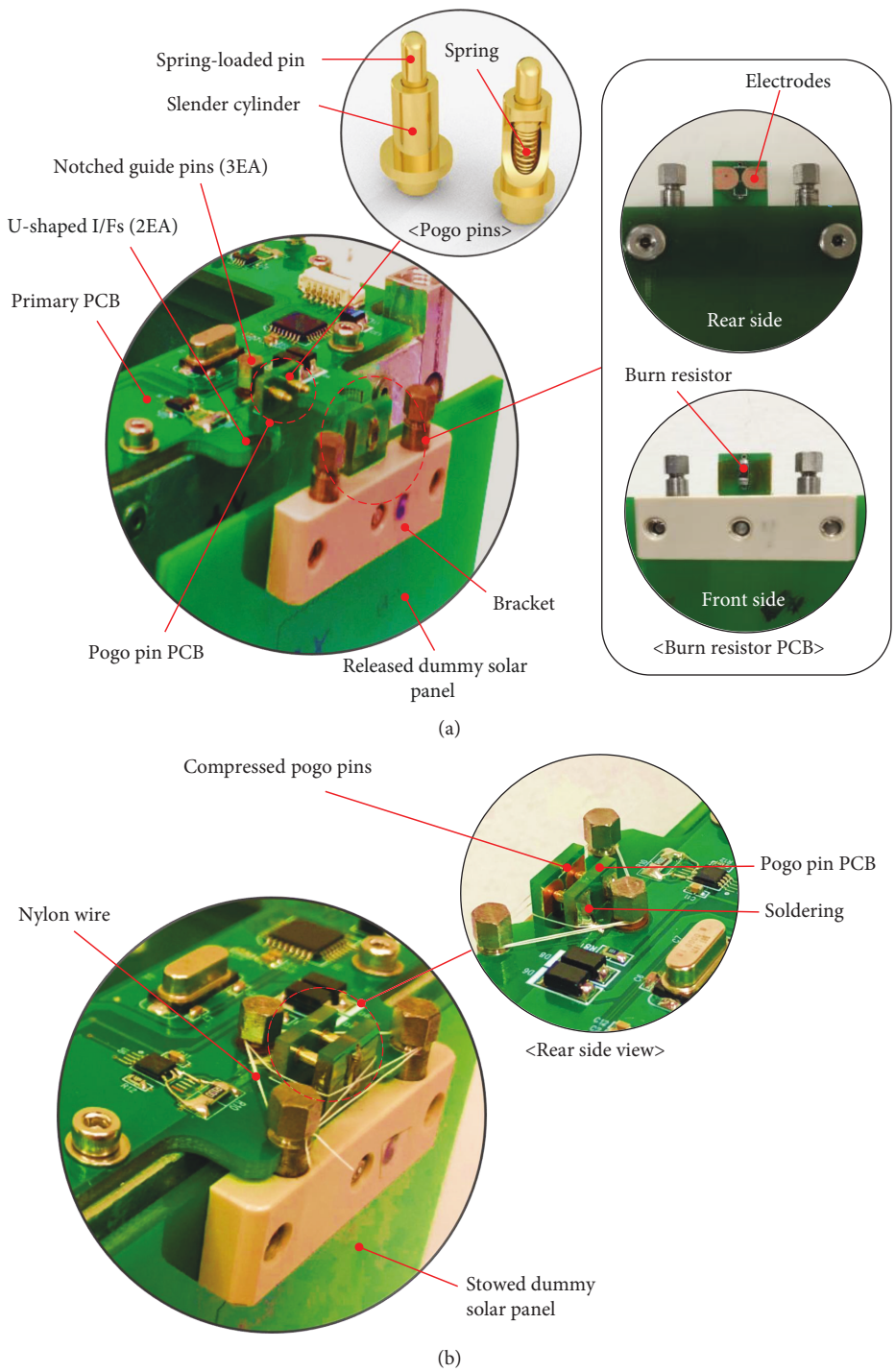

Figure 2: Enlarged configuration of pogo pin mechanism: (a) partially stowed and (b) fully stowed.

sinusoidal and random vibration tests. A TV test was also conducted to determine the survivability and reliability of the HRM in the simulated on-orbit thermal environment. The test results demonstrated that the proposed solar panel HRM was certified for use in actual space missions. The simple, reliable, and inexpensive HRM often contributes to significant cost reductions to a CubeSat program and aids in the success of space missions.

2. Pogo Pin-Based Holding and Release Mechanism for Deployable Solar Panel

Figure 1 shows the fully stowed and deployed configuration of the deployable solar panels for the 2U CubeSat, which is a development model, to validate the design feasibility of the modified pogo pin-based HRM. This model is mainly composed of a 2U dummy CubeSat structure, PCB, dummy

Table 1: Specifications of spring-loaded pogo pin.

Item	Details	Value
Spring-loaded pogo pin	Manufacturer	Hanbit T & I Co.
	Maximum allowable voltage and current	12 V, 2.0 A
	Contact resistance	Max. 30 mΩ
	Maximum number of loadings	30,000
	Operating temperature	-40°C to 85°C
	Operation power of spring-loaded pin	0.78 N ± 0.16 N

solar panels, and torsional hinges. The primary PCB with pogo pins positioned on the $+Z$ side of the CubeSat accommodates the electrical interface to provide power to the pogo pins and obtain deployment status signals for each solar panel during the activation of the mechanism. The simulated solar panel dummy PCBs made of FR4 with a thickness of 1.6 mm provide a mechanical interface for the integration of brackets and a burn resistor used for cutting through the nylon wires, which are mechanically connected with the primary PCB and dummy solar panels at the stowed position during launch.

Figures 2(a) and 2(b) show the closeup views of the pogo pin-based HRM with a partially and fully stowed solar panel, respectively. The proposed mechanism mainly consists of two spring-loaded pogo pins, a burn resistor, a support bracket, and three notched guide pins. The basic operating principle of the HRM proposed in this study is based on the nylon wire cutting method. However, the main feature of this mechanism, which differentiates it from the conventional mechanisms using the nylon wire cutting method, is the use of a spring-loaded pogo pin. The pogo pin is an electrical interface hardware that has been extensively used in the field of electronics for the implementation of a temporary connection between two electrical circuits. The pogo pin shown in Figure 2(a) is usually formed as a slender cylinder that contains a spring-loaded pin. When the spring-loaded pin is pressed between two electrical circuits, the tip of the pogo pin forms a secure contact between the two circuits by the restoring force acting on the spring-loaded pin. This function of a temporary electrical connection is useful for electrical applications, especially when many mating and demating cycles of the circuit are required. To demonstrate the function of the pogo pin on the proposed mechanism, two pogo pins were soldered on a pogo pin PCB that was vertically integrated in the primary PCB fixed by the soldering process, as shown in Figure 2(b). The implementation of the nylon wire cutting method requires the use of a heating element. Thus, a burn resistor was soldered on the front side of a burn resistor PCB, which was integrated in the dummy solar panel through the support bracket. The electrical pads, which are terminals connected with the resistor, are located on the rear side of the burn resistor PCB. The combination of the pogo pins and electrical pads achieves the temporary electrical connection to provide power to the resistor. Therefore, the proposed mechanism does not require an additional function to cut off the power to the resistor immediately after the release of the panels. Moreover, it prevents the failure of the burn resistor due to overheating by continuous provision of power after the panel release. In addition, the pogo pins also function as a status switch to detect the successful release of the solar panels by the observation of the electrical current flow status to the burn resistors. The restoring force of the spring-loaded pins also drives the initiation of the solar panel deployment. The multiple functions implemented by applying the pogo pin are advantageous for the proposed mechanism with respect to the simplicity of the system. Table 1 presents a detailed description of the spring-loaded pogo pin used in the qualification model of the mechanism.

The mechanical constraint along the out-of-plane direction of the solar panel is achieved by tightening the nylon wire along the three notched guide pins, as shown in Figure 2(b). Among these, two guide pins were fastened on the bracket mounted on the solar panel with the burn resistor PCB. Another guide pin was fastened on the rail structure of the dummy CubeSat through the hole interface of the primary PCB. When the solar panel is in the stowed position, the stroke of the spring-loaded pin should be within the nominal range, to ensure a reliable contact between the pogo pins and electrical pads on the burn resistor PCB. In the case of the pogo pin used in this study, the recommended stroke of the spring-loaded pin was 0.9 ± 0.1 mm. To meet the stroke requirement, the displacement limiters were implemented as U-shape interfaces at the edge of the primary PCB. The two notched guide pins mounted on the solar panel are combined with the U-shaped displacement limiter, when the solar panel is fully stowed. In addition, the U-shaped interface also provides the mechanical constraint along the in-plane direction of the solar panel. Thus, the proposed mechanism is more effective in securing the structural safety of the solar panel as the in-plane constraint implementation prevents the unintentional loosening of the nylon wire in the launch vibration environment. In the wire tightening process, the nylon wire was wound along the notches on the guide pins. These notches restrict the unexpected movement of the tightened nylon wire during the launch vibration environment, to ensure a stable contact with the burn resistor. Moreover, the knotting process of the nylon wire was performed on the corner area of one of the guide pins mounted on the solar panel. Therefore, the wire tightening process becomes much simpler and more reliable than the conventional wire cutting mechanisms, whose knotting process is performed on the flat surface of the solar panel. The release of the nylon cable winding along three notched guide pins is initiated by the activation of the burn resistor. For the

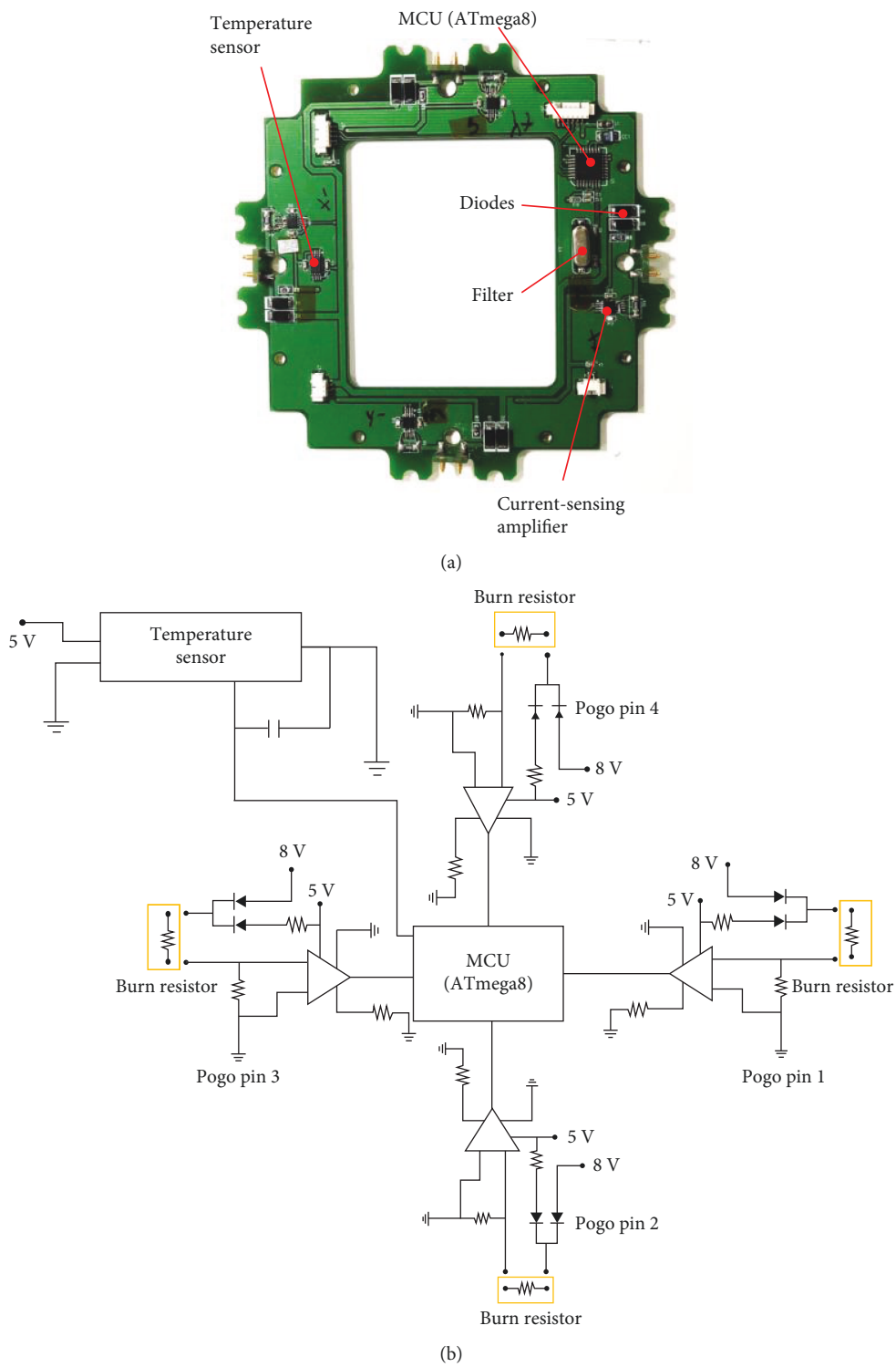

Figure 3: Configurations of primary PCB: (a) mechanical configuration and (b) electrical configuration.

deployment of the solar panels, as shown in Figure 1(b), the holding constraints achieved by the nylon wire tightening are released as the wire is cut, by applying power to the burn resistor. As compared with the conventional wire cutting mechanisms where the tightening process was performed on the flat surface, the proposed mechanism is much improved in terms of easier inspection and the tightening process. In particular, this also makes it easier to rework for the replacement of the damaged burn resistor during the on-ground test process.

Figures 3(a) and 3(b) show the mechanical and electrical configurations of the primary PCB, respectively. The

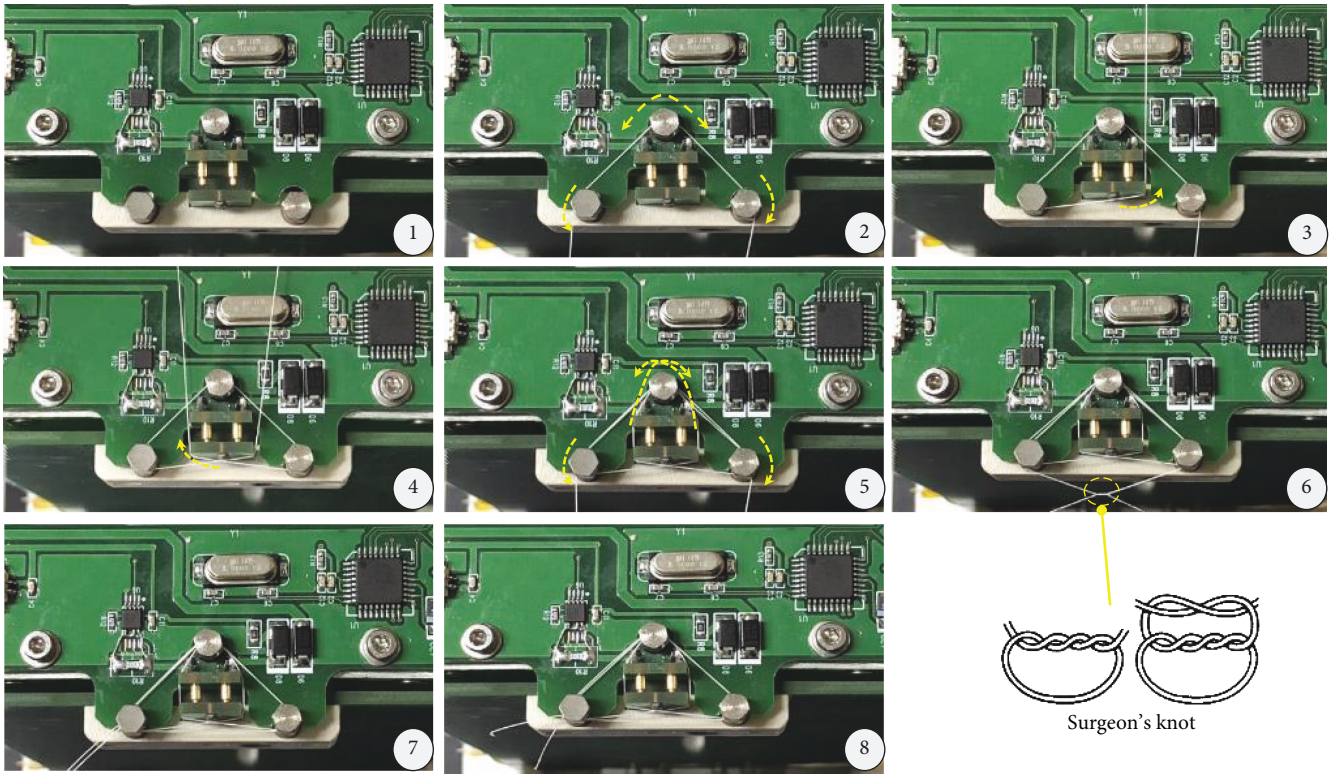

Figure 4: Tightening process of nylon wire.

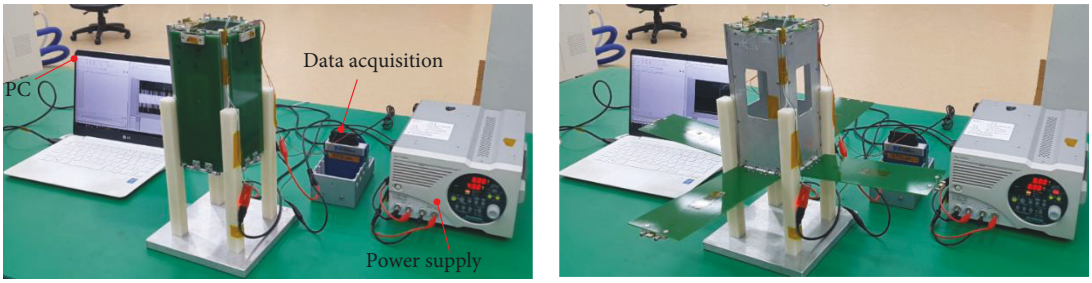

(a) (b)

Figure 5: Release function test setup: (a) before and (b) after deployment of solar panels.

primary PCB is mainly composed of an MCU, current sensing amplifiers (INA301), and a temperature sensor. To provide the electrical power to the burn resistors, the interfaces of the pogo pins applied for each solar panel were connected in parallel with an electrical power connector mounted on the PCB. This enables the synchronous release of multiple solar panels using a single power interface. The synchronous release capability is important for the minimization of the undesirable attitude tumbling of the CubeSat induced by the asymmetric panel deployment in its initial on-orbit stabilization phase. The input voltage for the activation of the mechanism was set to 8 V, which was validated to guarantee a reliable release of the solar panels in the previous study [13]. This voltage level can be sufficiently provided by the CubeSat power system using commercial Li-ion batteries. In the previous version of the pogo pin HRM [13], the function to detect the deployment status of the solar panels was not applied, as its main objective was to validate the feasibility of the mechanism. Therefore, in this study, the MCU combined with the current sensing amplifiers were added to the primary PCB to utilize the function of the pogo pins as the deployment status switches for the solar panels. Based on the current flow status to each burn resistor monitored by the current sensing amplifiers, the MCU provides a telemetry of "1" or "0" according to the stowage or deployment status of each solar panel. The temperature sensor provides the temperature status information of the primary PCB during its on-orbit operation. The panel cutout at the center of the PCB was intentionally implemented in the qualification model. This area allows to accommodate additional hardware such as a payload or other appendages. For the effective accommodation on the extremely limited area of the primary PCB, the electrical components were soldered on edges.

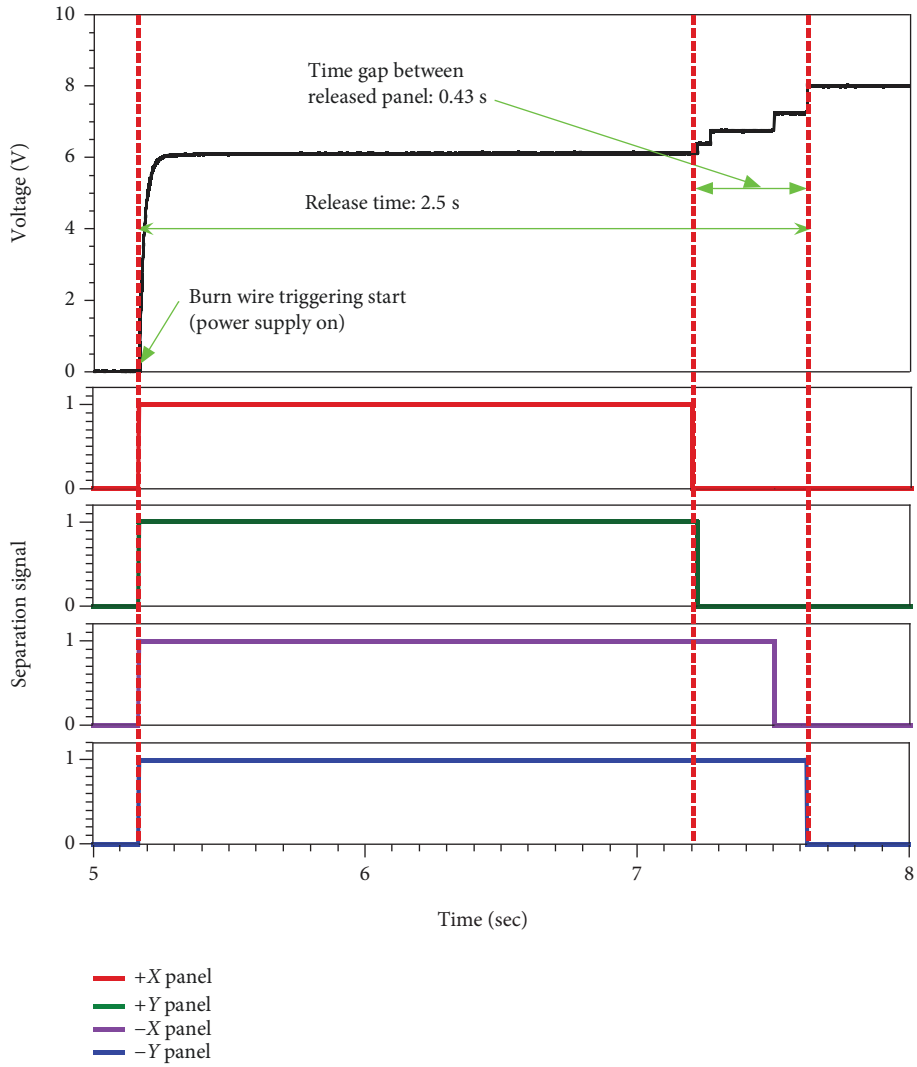

Figure 6: Time histories of input voltage and separation signals of each solar panel.

Figure 4 shows the tightening process of the nylon wire on the three notched guide pins shown in Figure 2(a). After winding the nylon wire along the guide pins and burn resistor, a knotting process of the nylon wire based on a surgeon knot was carried out on the corner surface of one of the guide pins. This optimized tightening process is simpler, and more effectively secures the solar panel in comparison with the conventional nylon wire cutting mechanisms whose wire tightening process is performed on the flat surface of the solar panel. The nylon wire (Berkley, Nanofil) [14] used in the proposed mechanism is made of fluorocarbon material with a diameter of 0.11 mm, which has a maximum allowable strength of 56.17 N. The nylon wire has an adequate strength and stiffness to endure the launch vibration environment and also has space heritage [15]. In addition, the test report [16] of the nylon wire stated that the elongation at the break of the wire decreases to 67.9% of the original value when it is exposed to the ultraviolet (UV) radiation expected in the space environment for 200 hrs. This indicates that the nylon wire has sufficient endurance against the UV environment taking into account that the deployment of the solar panel is typically initiated after several minutes to hours after the orbital injection of the CubeSat.

3. Results of Release Function Tests

To confirm the functionality of the proposed mechanism, release function tests were conducted with the experimental setup shown in Figure 5. The qualification model shown in Figure 1 was connected to a power supply to provide power for the mechanism activation and a data acquisition (DAQ) system to monitor the input power to the burn resistors and the deployment status signals from the solar panels during the test. The release function tests were performed according to the number of nylon wire windings, various temperature conditions, and repetitive activations of the mechanism.

Figure 6 shows the time histories of the input voltage to the burn resistors and separation signals of each solar panel monitored during the test. The release status data obtained

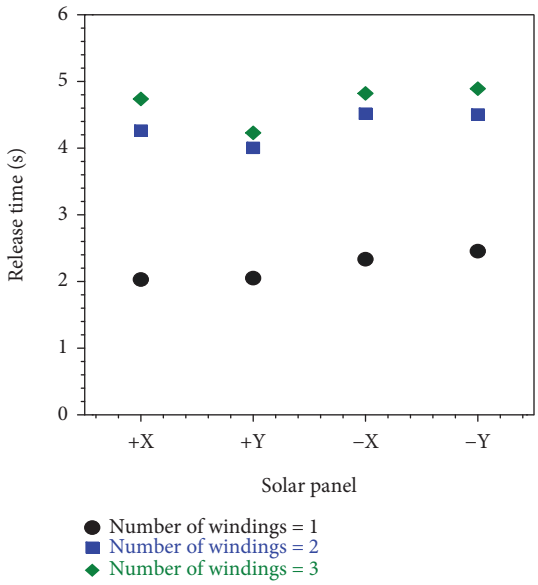

Figure 7: Release time of each solar panel according to the different numbers of nylon wire windings.

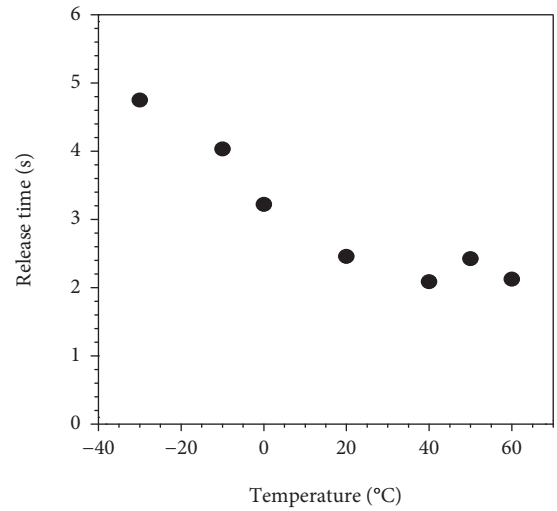

Figure 8: Variation in the release time of a solar panel under qualification temperature ranges.

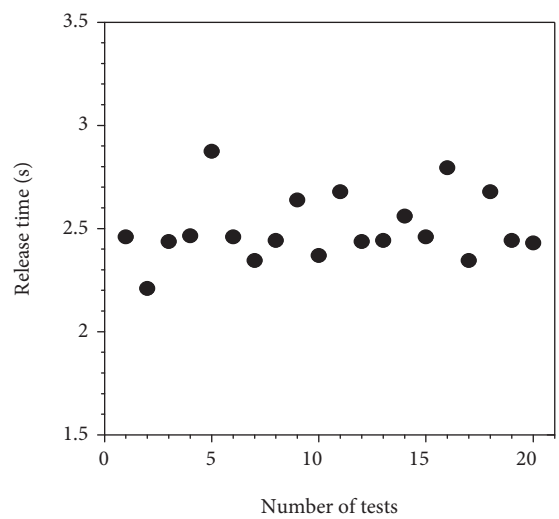

Figure 9: Variation in the release time of a solar panel during 20 times of repetitive release function tests at ambient temperature.

by the MCU indicated that all the solar panels were released within 2.5 s from the initiation of burn wire triggering, and the time gap between the released panels was at the maximum of 0.43 s. The test results indicated that the proposed mechanism guarantees the synchronous release of multiple solar panels. In addition, the MCU with a current sensing amplifier applied to the mechanism well detected the release status of each solar panel in accordance with the temporary electrical connection implemented by the pogo pins.

In this study, the 2U-sized dummy solar panel was applied to the qualification model shown in Figure 1. However, a higher holding capability might be required, as the size of the solar panel is increased. This can be achieved by changing the number of nylon wire windings. Thus, the release function test of the mechanism was conducted with different numbers of nylon wire windings. Figure 7 shows the release time of each solar panel with different numbers of nylon wire windings. The results indicated that the release time increases when the number of wire winding increases. The mechanism with the triple wire windings successfully released the constraint of the solar panel within 4.9 s, although this value is approximately two times higher compared with that of one wire winding. In addition, it still guaranteed a synchronous release of the multiple solar panels because the time gap between the released panels was only 0.83 s. These results indicate that the proposed mechanism also functions well with the application of multiple nylon wire windings.

The qualification temperature range of the mechanism ranges from -30°C to 60°C. The mechanism should function well under the given qualification temperature range, to assure its functionality in the on-orbit thermal environment. In particular, the mechanism could fail to release the panel constraint if the burn resistor is not sufficiently heated when it is exposed to the in-orbit low-temperature condition. Thus, release function tests were conducted under ambient temperature conditions. Figure 8 shows the variation in the release time of the solar panels under the qualification temperature ranges. The test results reveal that the release time increases in accordance with a decrease in temperature. However, the mechanism guarantees a reliable cut through within 5 s, even at the worst cold temperature of -30°C. These test results indicate that the mechanism functions well under specified qualification temperature ranges.

The repeatability of the mechanism is important because several numbers of release tests of the mechanism are required throughout the CubeSat development process. Thus, to validate the repeatability of the mechanism, the repetitive release function tests were performed, and the results are presented in Figure 9. The results indicate that the mechanism was operating well with no failure on the burn resistor during the repetitive activation of 20 times, although the release time was slightly varied due to the workmanship, to apply tension

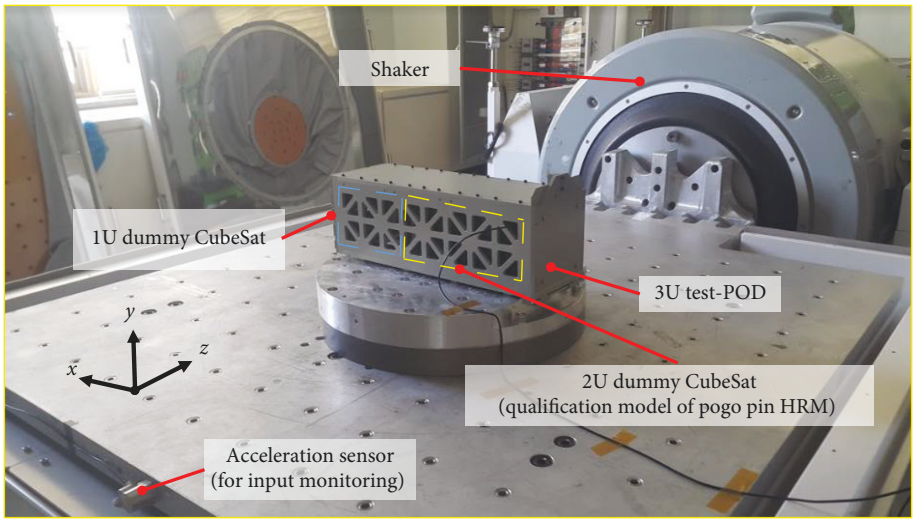

Figure 10: Example of vibration test setup of pogo pin HRM along the x-axis.

Table 2: Specifications of launch vibration test loads at qualification level.

(a) Sine vibration [18]

Level	Frequency (Hz)	Amplitude (g)	Sweep rate (oct/min)
0 dB (full level)	5	1.3	2
	8	2.5	
	100	2.5	

(b) Random vibration [19]

Level	Frequency (Hz)	Amplitude (g^2/Hz)	Duration (s)	RMS acceleration
0 dB (full level)	20	0.0260	120	14.10 G_{rms}
	50	0.1600		
	800	0.1600		
	2000	0.0260		

to the nylon wire during its tightening process. These results indicate that the mechanism assures sufficient repeatability for use in CubeSat applications.

4. Launch Vibration Test of Pogo Pin HRM

To verify the design effectiveness of the mechanism under a launch vibration environment, launch vibration tests were conducted at the qualification level. Figure 10 shows an example of a vibration test setup of the mechanism along the x-axis. The qualification model shown in Figure 1 was inserted into the 3U-sized test-picosatellite orbital deployer (Test-POD) with a 1U dummy CubeSat structure, to fill the residual space in the POD. The qualification test loads specified in Tables 2(a) and 2(b) were applied to the mechanism using an electrodynamics shaker (J260/SA7M, IMV Corp.). In the test, an accelerometer was attached to the test jig to measure the input test load. In addition, the acceleration responses at the dummy solar panels were obtained using the accelerometers attached to the center of the panels. The structural safety of the mechanism was evaluated by comparing the first eigenfrequency of the panels obtained through low-level sine sweep (LLSS) tests before and after each vibration test. After completing all the vibration tests, the release test of the solar panel was performed to evaluate the functionality of the mechanism.

Figure 11 shows the sine vibration test results along the x-axis. With respect to the amplitude of a sine vibration load of 2.5 g, the maximum acceleration responses of the $+X$ and $-X$ solar panels of 31.16 g and 28.42 g were observed at 77.2 Hz and 72.2 Hz, respectively. The 6.5% frequency difference between the $+X$ and $-X$ panels might be caused by the irregular workmanship during the tightening process of the nylon wire and the backlash on the rotational hinges. In general, these factors are inevitable when the nylon wire cutting type mechanism is used in CubeSat applications. Figure 12 shows the random vibration test results along the x-axis of the qualification model. In the test, the accelerometer at the

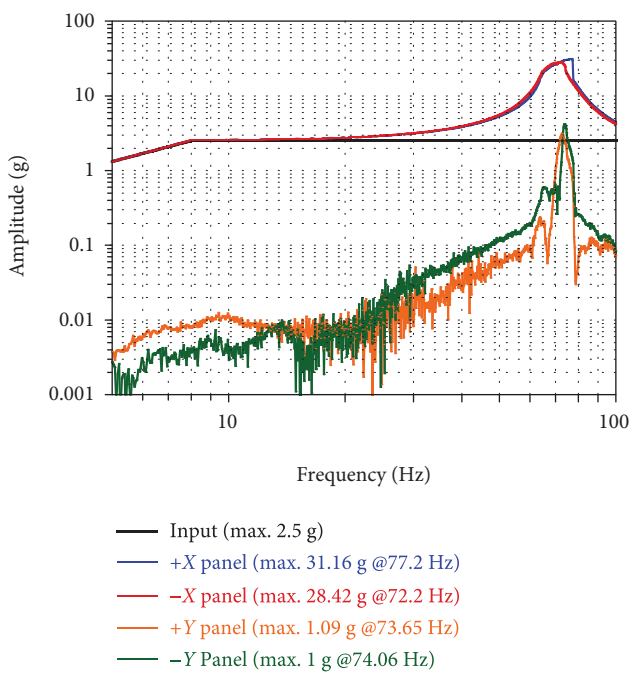

Figure 11: Sine vibration test results of the mechanism along the x-axis excitation.

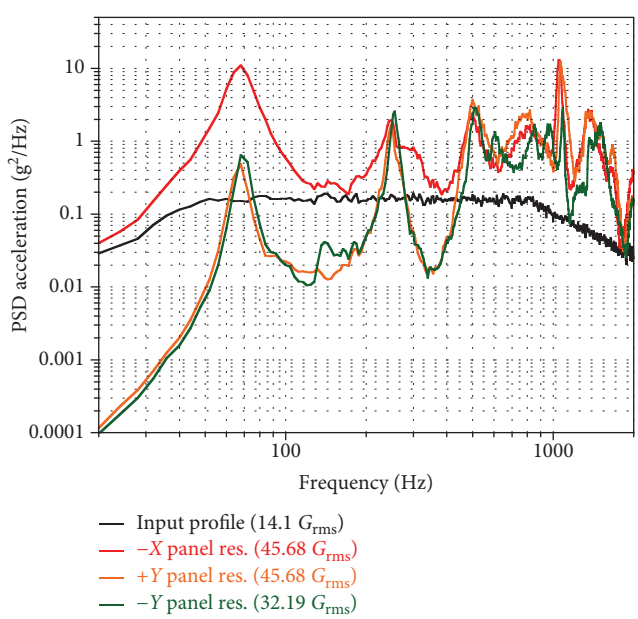

Figure 12: Random vibration test results of the mechanism along the x-axis excitation.

$+X$ panel was unintentionally detached from the panel surface, such that the response of the panel could not be obtained, although it was fully tested as specified in Table 2. The G_{rms} values of the $-X$, $+Y$, and $-Y$ panels calculated from the power spectral density (PSD) acceleration profiles were 45.68, 45.68, and 32.19 with respect to the test input of 14.1 G_{rms}. The maximum relative dynamic displacement at the center of the dummy panel, estimated from the vibration test results, was 1.68 mm. Therefore, the design configuration is within the ISIPOD [17] inner required dynamic clearance of 10 mm to avoid a crash between the P-POD interface and the solar cell.

Table 3: Representative LLSS test results before and after each vibration test.

Test axis	Status		1st eigenfrequency (Hz)	Difference (%)
x	$+X$ panel	Before	73.05	0.28
		After	72.84	
	$+Y$ panel	Before	72.84	0.27
		After	72.64	
y	$+X$ panel	Before	75.30	2.01
		After	73.81	
	$+Y$ panel	Before	74.06	0.06
		After	74.01	
z	$+X$ panel	Before	260.56	0.21
		After	260.02	
	$+Y$ panel	Before	273.84	1.50
		After	269.71	

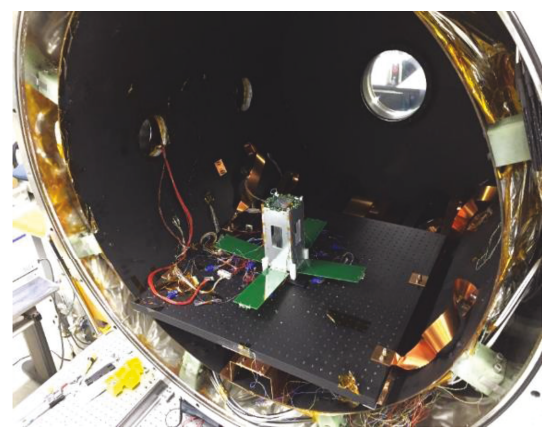

Figure 13: TV test setup after the release function test of the mechanism.

Table 3 summarizes the representative LLSS test results of the qualification model, i.e., the first eigenfrequencies of the $+X$ and $+Y$ panels before and after each vibration test. The requirement of the LLSS test is that the frequency shift to the dummy panel after the vibration test should be less than 5%. The table shows that the frequency shift was less than 2.01% throughout all the test sequences. These results indicate that the effectiveness of the proposed mechanism was successfully verified under the given qualification test loads.

5. Thermal Vacuum Test

Figure 13 shows the TV test setup to validate the functionality of the proposed mechanism under the space simulated TV environment, which was implemented in the ø1 m TV

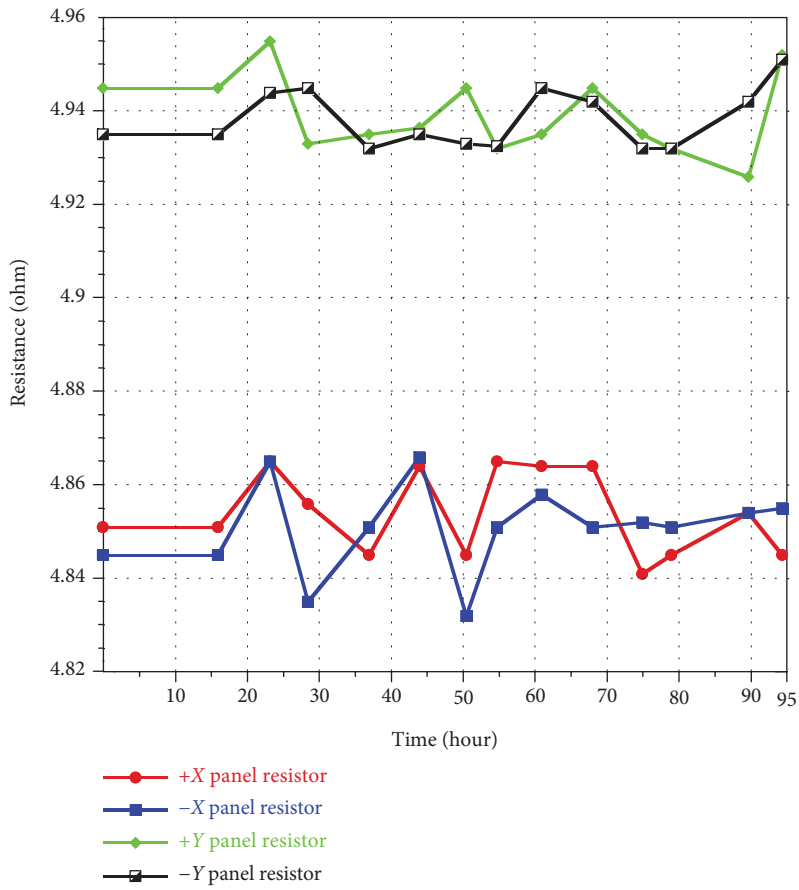

Figure 14: Variation in resistance values of the burn resistors during the TV test.

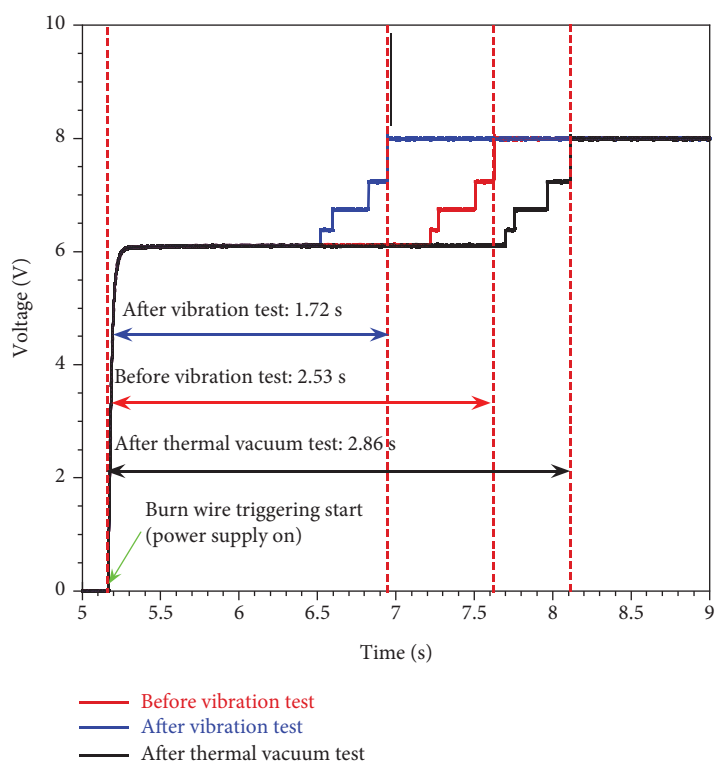

Figure 15: Comparison of the release time of the mechanism measured before the vibration test, after the vibration test, and after the TV test.

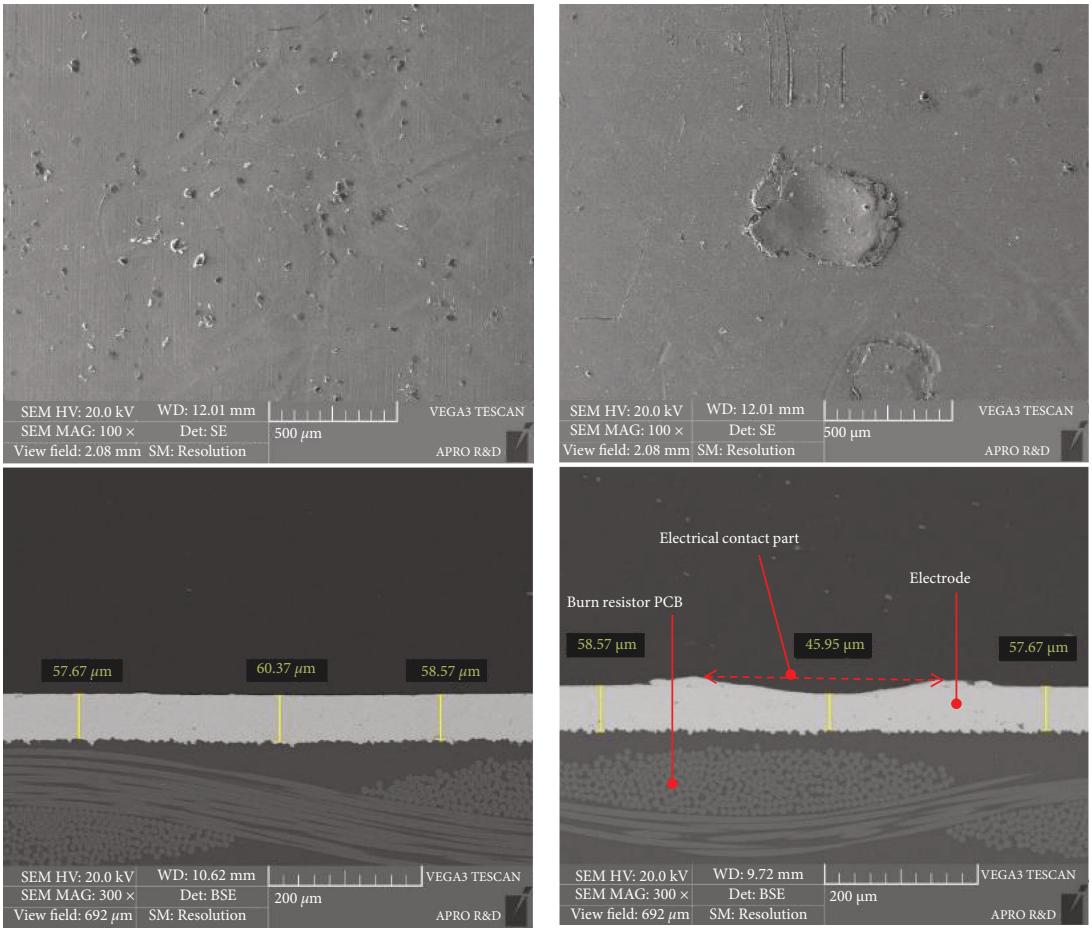

(a) (b)

Figure 16: SEM microphotographs of the electrodes of the burn resistor PCB: (a) pretest and (b) posttest.

chamber. A total number of 16 thermocouples were attached to the PCB and dummy panels. The temperature reference point (TRP) was located at the center surface of the dummy panel. The mechanism was exposed to a total number of six thermal cycles with the qualification temperature range from -30°C to 60°C under a chamber pressure less than 10^{-5} torr. The thermal dwell time at the hot and cold plateaus for a state of health (SOH) check of the mechanism was more than one hour and the required temperature change rate to declare the thermal equilibrium state of the hardware was less than 1°C per hour.

The SOH checks for the burn resistors were conducted on all the hot and cold soak phases, to check the survivability of the mechanism. Figure 14 shows the variation in the resistance values of the burn resistors measured during the TV test. The result indicates that the resistors exhibited the resistance variation of less than 0.7% throughout the test phases. This indicates that there was no performance degradation of the resistor during the TV test. Moreover, the release function test of the mechanism was performed in the 6th cold soak phase of the TV test as it was the worst condition for the mechanism activation. The test results confirmed that all the panels were successfully released as shown in Figure 13.

After the completion of the TV test, the release function test of the mechanism was also performed at ambient temperature conditions to confirm the functionality of the mechanism. The corresponding test results are presented in Figure 15. For comparison, the results obtained before and after the vibration test were also plotted in the figure. The panels were successfully released within 2.86 s, although there were differences of 13% and 66% with those measured before and after the vibration test, respectively. In addition, the time gap between the released panels was only 0.42 s. These observations indicate that the mechanism functioned well even after the launch vibration and TV tests.

In addition, when the dummy panel stowed and constrained by the mechanism is exposed to the launch and on-orbit environments, there is a possibility for the copper electrodes of the burn resistor PCB to be damaged due to the pressure applied by the sharp-edged tip of the pogo pins. This could lead to the degradation of the electrical contact between the burn resistor PCB and the pogo pins. Thus, scanning electron microscope (SEM) inspection was performed for the evaluation of the electrodes after completing all the qualification tests. Figure 16 shows the cross-sectional SEM microphotographs for the electrodes of the burn resistor PCB before and after exposure to the launch

vibration excitations. The thickness at the electrical contact part of the electrodes was 45.95 μm, which only had a 23.88% reduced value compared with the initial thickness. This means that a secure electrical contact would be guaranteed under the launch and on-orbit environments.

6. Conclusion

In this study, the qualification model of the pogo pin-based HRM with a redesigned electrical interface was developed and experimentally evaluated for use in the CubeSat deployable solar panel. The proposed mechanism is based on the nylon wire cutting method, but it provides an improved holding capability along the in-plane and out-of-plane directions of the solar panels, the synchronous release of multiple panels, and handling simplicity. The functionality of the mechanism was verified through the release function tests in ambient conditions, according to the number of repetitive activations, multiple nylon wire windings, and qualification temperature ranges. In addition, the structural safety of the mechanism was verified under simulated launch and on-orbit thermal environments. The release function tests conducted after the completion of the launch vibration and TV tests showed the nominal function of the mechanism. In addition, the SEM microscopic inspection results on the electrodes of the burn resistor PCB showed that the current design guarantees a secure electrical contact between the pogo pins and electrodes after exposure to the qualification loads. The results indicated that the proposed pogo pin-based HRM developed in this study was successfully qualified for use in CubeSat applications.

Data Availability

The data used to support the findings of this study are available from the corresponding author upon request.

Conflicts of Interest

The authors declare that there is no conflict of interest regarding the publication of this manuscript.

Acknowledgments

This work (Grant No. S2659457) was supported by the Business for Cooperative R&D between Industry, Academy, and Research Institute funded by the Korean Small and Medium Business Technology Administration in 2018.

References

[1] S. W. Janson, "The Future of Small Satellites," in *Small Satellites: Past, Present, and Future*, H. Helvajian and S. W. Janson, Eds., pp. 1–876, The Aerospace Press, El Segundo, CA, USA, 2008.

[2] F. Santoni, F. Piergentili, S. Donati, M. Perelli, A. Negri, and M. Marino, "An innovative deployable solar panel system for Cubesats," *Acta Astronautica*, vol. 95, pp. 210–217, 2014.

[3] P. A. Anigstein and R. S. Sanchez Pena, "Analysis of solar panel orientation in low altitude satellites," *IEEE Transactions on Aerospace and Electronic Systems*, vol. 34, no. 2, pp. 569–578, 1998.

[4] F. Santoni, F. Piergentili, G. P. Candini, M. Perelli, A. Negri, and M. Marino, "An orientable solar panel system for nanospacecraft," *Acta Astronautica*, vol. 101, pp. 120–128, 2014.

[5] J. Armstrong, C. Casey, G. Creamer, and G. Dutchover, "Pointing control for low altitude triple Cubesat space darts," in *23th Annual AIAA/USU Small Satellite Conference*, pp. 1–8, Logan, UT, USA, 2009.

[6] J. Bouwmeester, G. Brouwer, E. Gill, G. Monna, and J. Rotteveel, "Design status of the Delfi-Next nanosatellite project," in *61st International Astronautical Congress*, pp. 1–13, Prague, Czech Republic, 2010.

[7] T. Jansen, A. Reinders, G. Oomen, and J. Bouwmeester, "Performance of the first flight experiment with dedicated space CIGS cells onboard the Delfi-C3 nanosatellite," in *2010 35th IEEE Photovoltaic Specialists Conference*, pp. 20–25, Honolulu, HI, USA, 2010.

[8] J. M. Plaza, J. A. Vilan, F. A. Agelet et al., "Xatcobeo: small mechanisms for CubeSat satellites—antenna and solar array deployment," in *Proceedings of the 40th Aerospace Mechanisms Symposium*, pp. 415–429, Cocoa Beach, FL, USA, 2010.

[9] H. U. Oh, M. S. Jo, K. M. Lee, and D. J. Kim, "Spaceborne tilt mirror mechanism and application of shape memory alloy actuator to implement fail-safe function in emergency mode," *Transactions of the Japan Society for Aeronautical and Space Sciences*, vol. 55, no. 6, pp. 373–378, 2012.

[10] H. Yano, T. Kubota, H. Miyamoto et al., "Touchdown of the Hayabusa spacecraft at the Muses Sea on Itokawa," *Science*, vol. 312, no. 5778, pp. 1350–1353, 2006.

[11] A. Thurn, S. Huynh, S. Koss et al., "A nichrome burn wire release mechanism for CubeSats," in *Proceedings of the 41st Aerospace Mechanisms Symposium*, pp. 479–488, Pasadena, CA, USA, 2012.

[12] H. U. Oh and M. J. Lee, "Development of a non-explosive segmented nut-type holding and release mechanism for cube satellite applications," *Transactions of the Japan Society for Aeronautical and Space Sciences*, vol. 58, no. 1, pp. 1–6, 2015.

[13] T. Y. Park, S. H. Kim, H. Kim, and H. U. Oh, "Experimental investigation on the feasibility of using spring-loaded pogo pin as a holding and release mechanism for CubeSat's deployable solar panels," *International Journal of Aerospace Engineering*, vol. 2018, Article ID 4854656, 10 pages, 2018.

[14] http://www.berkley-fishing.com/berkley-line-uni-filament-berkley-nanofil/berkley-nanofil/1285551.html.

[15] K. Nakaya, K. Konoue, H. Sawada et al., "Tokyo Tech Cubesat: CUTE-I—design & development of flight model and future plan," in *AIAA 21st International Communications Satellite Systems Conference and Exhibit*, pp. 1–10, Yokohama, Japan, 2003.

[16] P. Platzer and G. Grantham, "UV weathering & tensile tests on nanofil & vantage lines," F5144, Spire Global UK Ltd, 2015.

[17] https://www.isispace.nl/product/isipod-cubesat-deployer.

[18] F. Singarayar, R. Reinhard, C. Asma et al., "QB50 system requirements and recommendations," Issue 4, 2013, http://www.qb50.eu.

[19] "General environmental verification standard (GEVS) for GSFC flight programs and projects," GSFC-STD-7000A, NASA Goddard Space Flight Center, 2013.